Solution properties of poly(vinylidene fluoride): 1. Macromolecular characterization of soluble samples

G. Lutringer* and G. Weill
Institut Charles Sadron (CRM-EAHP), Université L. Pasteur, 6 rue Boussingault, 67083 Strasbourg Cedex, France
(Received 7 November 1989; revised 22 February 1990; accepted 27 April 1990)

Dissolution in a range of solvents reveals two kinds of behaviour of poly(vinylidene fluoride) (PVDF): readily soluble samples (mostly suspension-polymerized) and partly gel-forming samples (mostly emulsion-polymerized). From molecular characterization of a number of industrial and laboratory samples of the first kind in solution in different solvents by light scattering, intrinsic viscosity and size exclusion chromatography, we derive unperturbed dimensions and χ parameters. Our results differ from previous measurements where light-scattering experiments were carried out in solvents with very low dn/dc and/or on less-soluble (second-kind) PVDF, where microgel formation cannot be avoided.

(Keywords: poly(vinylidene fluoride); conformation; thermodynamic interaction; light scattering; intrinsic viscosity; size exclusion chromatography)

INTRODUCTION

Poly(vinylidene fluoride) (PVDF) has been extensively studied in the solid state to relate its structure to its piezoelectric properties[1]. Only a few studies, however, have been directed towards the molecular-mass and solution properties of PVDF. Stillwagon[2] has reviewed the early intrinsic viscosity $[\eta]$ *versus* molecular mass relations proposed by Welch[3] for PVDF in dimethylacetamide (DMAc) at 25°C and by Ali and Raina[4] for PVDF in dimethylformamide (DMF), *N*-methylpyrrolidone (NMP) and DMAc at 125°C. Stillwagon's own measurements deal with NMP solutions at room temperature. His light-scattering experiments have been carried out on industrial samples from Pennwalt Corp. (Kynar) and Kureha Chemical Industry Co. (KF) using a Chromatix KMX6 low-angle light-scattering instrument. The very low scattering volume allows one to filter out in the signal the sharp spikes due to the presence of 'foreign particles' and to obtain the true scattering of the solution. As a result, the measured molecular mass is much lower than obtained by an application of the Mark–Houwink relation given by Welch or Ali and Raina to the measured intrinsic viscosity. This in turn cast some doubt on the unperturbed dimensions and characteristic ratio C_∞ proposed by these authors.

There are several difficulties in performing light-scattering (LS) experiments on PVDF solutions: low increments of index of refraction dn/dc in DMF and DMAc, possible dehydrofluorination leading to some fluorescence (NMP and acetophenone[3] at high temperatures) and presence of microgel.

In a systematic study of the solubility and molecular mass of industrially produced emulsion- or suspension-polymerized PVDF samples, it became progressively clear that some samples (type I PVDF hereafter) are readily soluble in solvents such as DMF, DMAc and NMP, while other samples (type II PVDF hereafter) form microgels in the same solvents.

The relation between the solubility and the microstructure of these two classes of PVDF is the object of another paper (part 2[5]). In this part 1 we take advantage of the solubility of type I PVDF to achieve a complete molecular characterization in solution. In the next section we deal with the choice of samples and solvents. Then we report the LS and $[\eta]$ measurements, and the size exclusion chromatography (s.e.c.) experiments and the conversion from the equivalent molecular masses from polystyrene (PS) or poly(ethylene oxide) (PEO) standards to true molecular masses. As we have controlled the sample polymolecularity, we are able to derive the thermodynamic interaction parameters and unperturbed dimensions in the different solvents.

SAMPLES, SOLVENTS AND EXPERIMENTAL PROCEDURES

Several industrial type I PVDF samples have been used, from Daikin (VP800, VP810), Dynamit Nobel (Dyflor 2000M), Kureha (KF1000) and Solvay (Solef S1010 and S1012), without further purification. To broaden the range of available molecular masses, a series of samples labelled A1 to A9 have been prepared by Atochem.

A search for good solvents with sufficiently high dn/dc by inverse chromatography and $[\eta]$ measurements has been reported elsewhere[6]. It led us to select 1,3-dimethyl-2-oxohexahydropyrimidine (*N*,*N*'-dimethyl-*N*,*N*'-trimethylene urea (DMPU)) as the most suitable good solvent. A few experiments have also been carried out with the carcinogenic solvent hexamethylphosphotriamide (HMPT). Dimethylsulphoxide (DMSO) has been used as a bad solvent with high dn/dc. The values of dn/dc measured in the above at 546 and 633 nm using

* Present address: Ciba-Geigy, Basel, Switzerland

0032-3861/91/050877-07

Table 1 Refractive-index increment of PVDF in several solvents at 25°C

Solvent	n_D	dn/dc (cm^3 g^{-1}) At $\lambda = 632$ nm	dn/dc (cm^3 g^{-1}) At $\lambda = 546$ nm
DMF	1.4305	−0.021	−0.023
DMAc	1.438	−0.031	−0.033
NMP	1.468	−0.050	−0.052
HMPT	1.458	−0.044	−0.046
DMSO	1.477	−0.060	−0.062
DMPU	1.489	−0.065	−0.067

a Brice-Phoenix differential refractometer are given in *Table 1* together with those in DMF, DMAc and NMP.

Light-scattering experiments have been carried out at room temperature on centrifuged solutions with a Fica instrument equipped with either a high-pressure mercury lamp ($\lambda = 546$ nm) or a He–Ne laser ($\lambda = 633$ nm). The analysis of the results according to the Zimm plot procedure takes care of the polarization of the source[7]. It provides the weight-average molecular mass M_w, the z-average mean-square radius of gyration $\langle s^2 \rangle_z$ and the second virial coefficient A_2. A typical Zimm plot is given in *Figure 1*.

Intrinsic viscosity measurements have been carried out in a Fica automatic Ubbelohde viscometer at 25°C. All solutions have been previously filtered on sintered glass. Intrinsic viscosity $[\eta]$ and Huggins constants k have been calculated from a linear regression on times of flow t according to:

$$(t - t_0)/t_0 c = [\eta](1 + k[\eta]c) \quad (1)$$

where t_0 is the time of flow of the solvent and c the sample concentration.

Size exclusion chromatography has been performed at Atochem Research Center on their Waters instruments. Styragel columns were used with DMF at 95°C as solvent and Shodex 80 M columns with NMP/10^{-1} M LiBr at 85°C as solvent. Calibration was performed with PEO and PS standards. A check for full recovery of the injected polymer has been performed from the area of the refractometric signal.

A double detection with either a viscosimetric or a low-angle LS detector has been made available to us in a selected number of cases.

RESULTS FROM LIGHT SCATTERING AND INTRINSIC VISCOSITY

Values of M_w, $\langle s^2 \rangle_z$ and A_2 in different solvents are reported in *Table 2*. The agreement between values of M_w in different solvents is very satisfactory. The estimated errors result from repeated experiments.

Intrinsic viscosities $[\eta]$ and Huggins constants k are reported in *Table 3*. The values of k appear somewhat low compared to values generally accepted (0.4).

From the variation of $\langle s^2 \rangle_z$, $[\eta]$ and A_2 from one solvent to the others, it is easy to give the following order of solvent quality:

$$\text{DMSO} < \text{DMF} < \text{DMAc} < \text{NMP} \simeq \text{HMPT} \simeq \text{DMPU}$$

Log–log plots of $\langle s^2 \rangle_z$ *versus* M_w (*Figure 2*) and A_2 *versus* M_w (*Figure 3*) provide power laws (*Table 4*):

$$\langle s^2 \rangle_z = A M_w^{2\nu} \quad (2)$$

$$\langle A_2 \rangle = B M_w^{\nu'} \quad (3)$$

with exponents ν and ν' that clearly reflect the progression in solvent quality. The situation is less clear with $[\eta]$ *versus* M_w plots (*Figure 4*): the points are more scattered and the intrinsic viscosity of the higher-molecular-mass sample is nearly independent of the solvent. The corresponding Mark–Houwink laws:

$$[\eta] = k M^a \quad (4)$$

are somewhat ill-defined and the sense of variation of a calculated from a linear regression contradict the variation observed in the absolute values of $[\eta]$ (*Table 4*). Within ±6% experimental accuracy, however, all results in good solvents would fit:

$$[\eta] = (4.5 \pm 0.3) \times 10^{-4} M_w^{0.70} \quad (5)$$

It is compared in *Figure 4* with the results of Welch[3] in DMAc and Ali and Raina[4] in DMF at 125°C. While there is no difference in the slope, the values of k are not consistent with ours by a factor of ~0.5 for ref. 3 and ~10 for ref. 4. This may be due both to difficulties in the light-scattering experiments and to large differences in polymolecularity.

We therefore defer the discussion on scaling laws until after the characterization of sample polymolecularity by s.e.c.

RESULTS FROM SIZE EXCLUSION CHROMATOGRAPHY

S.e.c. in DMF

First experiments have been carried out at Atochem[8] in DMF at 95°C using four columns of porosity 10^6, 10^5, 10^4, 10^3 Å. Apparent average molecular masses $M_{w,PEO}$ and $M_{w,PS}$ and polymolecularity indices $I_p = M_w/M_n$ and $I_{p+1} = M_z/M_w$ have been calculated according to PEO and PS calibration. They are reported in *Table 5* together with the 'true' M_w obtained by LS. We can notice that:

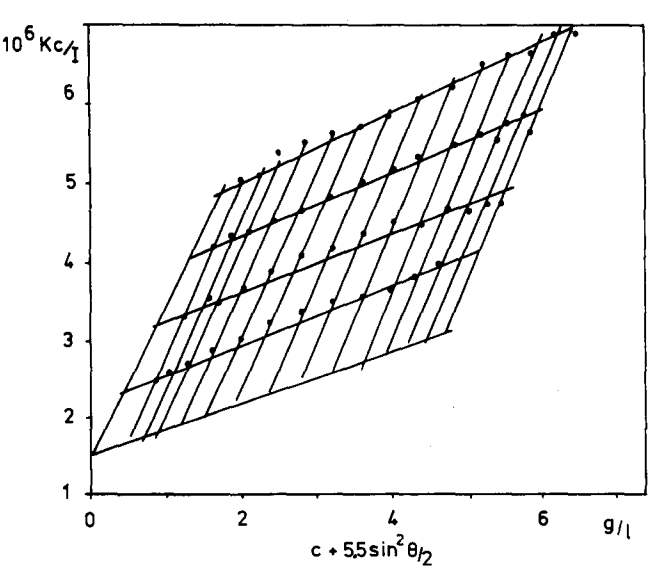

Figure 1 Zimm plot of PVDF sample A9 in DMPU ($M_w = (700 \pm 11) \times 10^{-3}$ g mol^{-1}, $\langle s^2 \rangle_z^{1/2} = 75.6 \pm 5.5$ nm, $10^5 A_2 = 99$ mol cm^3 g^{-2})

Table 2 Light scattering in different solvents (M_w = weight-average molecular mass (g mol^{-1}), $\langle s^2\rangle_z$ = z-average radius of gyration (nm), A_2 = second virial coefficient (mol cm^3 g^{-2}))

	DMSO			DMF			DMAc		
Sample	$10^{-3}M_w$	$\langle s^2\rangle_z^{1/2}$	10^5A_2	$10^{-3}M_w$	$\langle s^2\rangle_z^{1/2}$	10^5A_2	$10^{-3}M_w$	$\langle s^2\rangle_z^{1/2}$	10^5A_2
A1	105 ± 5	14.8 ± 3.0	5	114 ± 11	18.1 ± 4.0	15	104 ± 8	20.2 ± 3.5	100
A2	113 ± 6	15.6 ± 3.0	5	118 ± 10	18.7 ± 4.2	16	115 ± 9	21.5 ± 3.6	100
A3	135 ± 7	16.7 ± 3.5	4	148 ± 12	21.1 ± 4.4	12	140 ± 10	24.5 ± 4.0	90
A4	140 ± 7	17.2 ± 3.5	4	156 ± 12	22.1 ± 4.2	12	138 ± 10	24.0 ± 4.0	87
A5	158 ± 8	18.3 ± 3.5	4	175 ± 13	23.3 ± 4.2	11	155 ± 11	26.0 ± 3.5	87
A6	160 ± 10	19.1 ± 3.7	4	160 ± 14	22.1 ± 4.1	11	158 ± 10	26.5 ± 3.4	81
S1010	170 ± 12	20.2 ± 3.0	3	163 ± 15	22.4 ± 4.3	12	165 ± 12	27.0 ± 3.2	83
A7	200 ± 16	21.0 ± 3.0	2	218 ± 14	26.5 ± 4.2	10	205 ± 12	30.8 ± 3.6	71
S1012	220 ± 18	22.6 ± 3.4	1	235 ± 15	27.6 ± 4.4	9	238 ± 14	33.4 ± 3.3	68
A8	322 ± 20	26.5 ± 3.0	1	325 ± 8	33.4 ± 4.8	8	326 ± 16	40.3 ± 5.3	59
A9	700 ± 70	40.7 ± 5.0	−1	710 ± 8	50.3 ± 5.2	7	695 ± 17	62.0 ± 6.0	42
	NMP			DMPU			HMPT		
Sample	$10^{-3}M_w$	$\langle s^2\rangle_z^{1/2}$	10^5A_2	$10^{-3}M_w$	$\langle s^2\rangle_z^{1/2}$	10^5A_2	$10^{-3}M_w$	$\langle s^2\rangle_z^{1/2}$	10^5A_2
A1	102 ± 5	21.7 ± 4.0	126	96 ± 3	22.0 ± 3.5	150	103 ± 3	23.0 ± 3.0	180
A2	111 ± 6	22.8 ± 3.7	124	112 ± 3	24.2 ± 4.0	145			
A3	131 ± 7	25.2 ± 4.0	105	132 ± 4	26.5 ± 4.0	135			
A4	141 ± 7	26.5 ± 4.2	103	139 ± 4	27.9 ± 4.0	125			
A5	152 ± 8	27.9 ± 4.3	105	155 ± 4	29.9 ± 4.0	125			
VP810				153	30	125			
A6	154 ± 8	28.0 ± 4.0	115	156 ± 4	30.2 ± 4.0	125			
S1010	171 ± 7	29.6 ± 3.6	110	173 ± 4	31.4 ± 4.0	132			
A7	200 ± 6	33.0 ± 3.4	110	200 ± 4	34.7 ± 4.0	129	199 ± 5	35.4 ± 4.3	160
D2000				200 ± 5	36	128			
S1012	238 ± 7	36.5 ± 4.0	103	232 ± 5	38.0 ± 4.0	115			
A8	310 ± 10	44.1 ± 5.0	100	322 ± 6	46.9 ± 5.0	110			
A9	702 ± 20	74.2 ± 6.0	88	700 ± 11	76.5 ± 5.5	99	698 ± 12	73.8 ± 5.0	120
KF1000				151	29.5	130			
VP800				145	29	125			

Table 3 Intrinsic viscosities $[\eta]$ (dl g^{-1}) and Huggins constants k

	DMF		DMAc		NMP	DMPU
Sample	$[\eta]$	k	$[\eta]$	k	$[\eta]$	$[\eta]$
A1	0.74	0.31	0.76	0.35	0.81	0.92
A5			1.14	0.4		
S1010			1.16	0.37		
A7	1.28	0.36	1.43	0.32	1.45	1.51
A8	1.75	0.39	1.89	0.27	1.98	2.1
A9			3.25	0.42	3.30	3.4

(i) the good agreement between $M_{w,PEO}$ and the true M_w ($M_{w,PS}$) is roughly twice as large in the range explored;
(ii) the good agreement between I_p or I_{p+1} for both calibrations; and
(iii) the rather uniform polymolecularity for the different samples.

Application of universal calibration. Universal calibration[7] associates with the elution volume a value of the hydrodynamic volume that is proportional to $[\eta]M$. Thus one can convert apparent M_w to true M_w provided that the Mark–Houwink relation in the solvent used for s.e.c. is known for both the standard (index 1) and the polymer (index 2) under study. In that case for each molecular mass:

$$M_2 = \frac{K_1}{K_2} M_1^{\left(\frac{1+a_1}{1+a_2}\right)} = SM_1^t \tag{6}$$

If $t \simeq 1$ relation (6) holds for any average molecular mass. This requires $a_1 = a_2$, i.e. the solvent is equally good for polymers 1 and 2. The polymolecularity index then remains unchanged by the conversion.

When the Mark–Houwink relation is unknown, Mori[9] has proposed to derive relations (5) and (6) from the chromatograms of two samples with sufficiently different M_w accurately known from LS. If h_{zi} is the height of the chromatogram associated with the elution volume corresponding to the molecular mass M_{1i} of the standard:

$$M_{w2} = \frac{\sum h_{zi} S M_{1i}^t}{\sum h_{zi}} \tag{7}$$

A numerical search on two well known samples provides S and t. Application to samples A1 ($M_w = (105 \pm 9) \times 10^3$) and A7 ($M_w = (205 \pm 10) \times 10^3$) provided us with:

PEO calibration	$S = 4.46$,	$t = 0.87$
PS calibration	$S = 3.15$,	$t = 0.85$

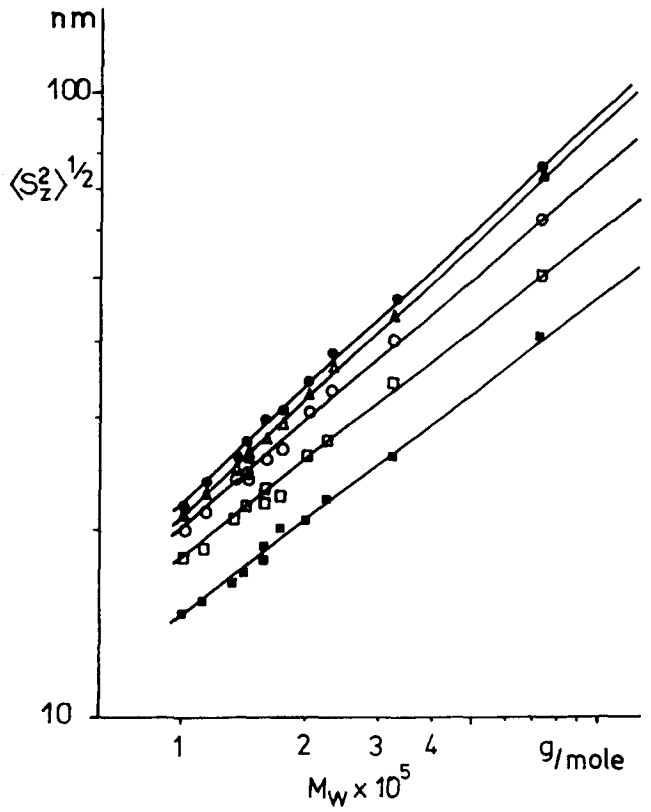

Figure 2 Plot of $\langle s^2 \rangle_z^{1/2}$ as a function of M_w (g mol^{-1}). The solvents are DMSO (■), DMF (□), DMAc (○), NMP (△) and DMPU (●)

The low values of t make the result very suspicious since we expect here $a_1 > a_2$ (i.e. $t > 1$), and so we have not pursued the procedure for converting $M_{w,PS}$ to true M_w, since $M_{w,PEO}$ appears directly as very close to it.

S.e.c. in NMP/LiBr at 80°C

$M_{w,PEO}$ and I_p for a few samples are given in *Table 6*. The agreement with the true M_w from LS again appears very good. The application of Mori's procedure gives $S = 0.81, t = 1.01$. The polymolecularity index I_p appears, however, rather high when compared to experiments in DMF. This can be related to the poor solubility of PEO in NMP, which makes the calibration curve for high molecular masses doubtful.

$M_{w,PS}$ is much larger than true M_w from LS but the I_p are much closer to that observed in DMF (*Table 5*). Mori's procedure gives $S = 1.4$ and $t = 0.96$, a value close

Table 4 Parameters of the scaling laws for the mean-square radius of gyration $\langle s^2 \rangle_z$, the second virial coefficient A_2 and the intrinsic viscosity $[\eta]$ according to relations (2), (3) and (4)

Parameter	DMF	DMSO	DMAc	NMP	DMPU
ν	0.51	0.53	0.57	0.62	0.62
$10^2 B$	1.6	1.2	10	1.2	1.5
ν'	−0.5	−0.4	−0.4	−0.2	−0.2
$10^4 k$	1.95		2.15	3.27	6
a	0.73		0.715	0.69	0.645

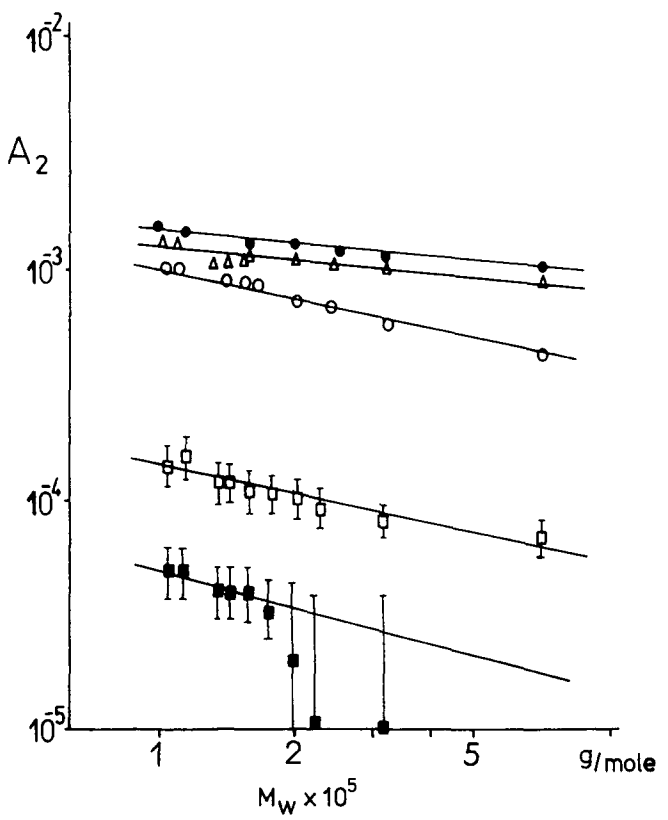

Figure 3 Plot of A_2 (cm^3 g^{-2} mol) as a function of M_w (g mol^{-1}); same symbols as in *Figure 2*

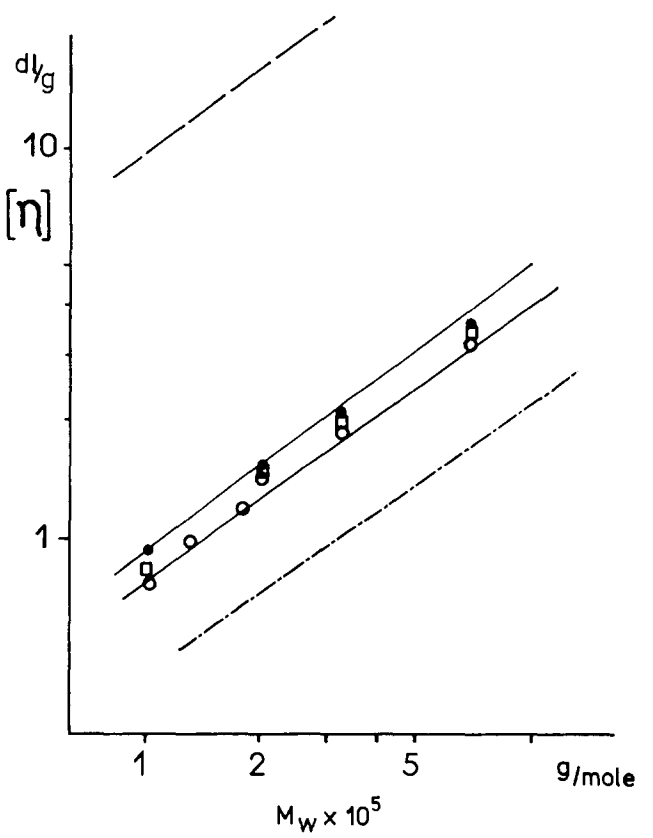

Figure 4 Plot of $[\eta]$ as a function of M_w (g mol^{-1}); same symbols as in *Figure 2*. Full lines show that the experiments can be fitted with an average value of $a = 0.70$ within experimental error for all good solvents. The chain line is the Mark–Houwink relation of ref. 3 (DMAc); and the broken line is that of ref. 4 (DMF at 125°C)

Table 5 S.e.c. results in DMF. I_p and I_{p+1} are the polymolecularity indices M_w/M_n and M_z/M_w

	LS	S.e.c. (PEO)			S.e.c. (PS)		
Sample	$10^{-3}M_w$ (g mol^{-1})	$10^{-3}M_w$ (g mol^{-1})	I_p	I_{p+1}	$10^{-3}M_w$ (g mol^{-1})	I_p	I_{p+1}
A1	96	110	2.7	2.5	227	2.5	2.6
A2	112	112	2.3	2.4	233	2.1	2.4
A3	132	144	3.2	3	241	2.8	2.4
A5	155	168	2.5	2	236	2.1	1.8
S1010	173	149	2.4	2.2	305	2.3	2.2
A7	200	225	2.6	2.4	450	2.3	2.4
S1012	232	241	3.1	2.7	481	2.8	2.5

Table 6 S.e.c. results in NMP/LiBr at 85°C

	LS	S.e.c. (PS)			S.e.c./LS	S.e.c./[η]	S.e.c. (PEO)		
Sample	$10^{-3}M_w$ (g mol^{-1})	$10^{-3}M_w$ (g mol^{-1})	I_p	I_{p+1}	$10^{-3}M_w$ (g mol^{-1})	$10^{-3}M_w$ (g mol^{-1})	$10^{-3}M_w$ (g mol^{-1})	I_p	I_{p+1}
A1	96	137	2.1	2.6	98	90	92	3.3	3.2
A2	112	150	1.9	2.3					
A4	140	175	1.9	2.0					
VP800	145	190	2.0	2.0					
A5	155	217	2.0	1.6	153	140			
KF1000	151	225	1.9	2.0					
VP810	153	228	2.2	2.1		144	152	2.6	2.5
S1010	173	240	2.0	2.4		140			
A7	200	280	2.0	2.1	197	175	198	2.5	2.4
D2000	200	287	2.0	2.1					
S1012	232	308	2.3	2.2					
A8	322	370	2.1	2.3	317				
A9	700	695	2.6	2.6	700	650			

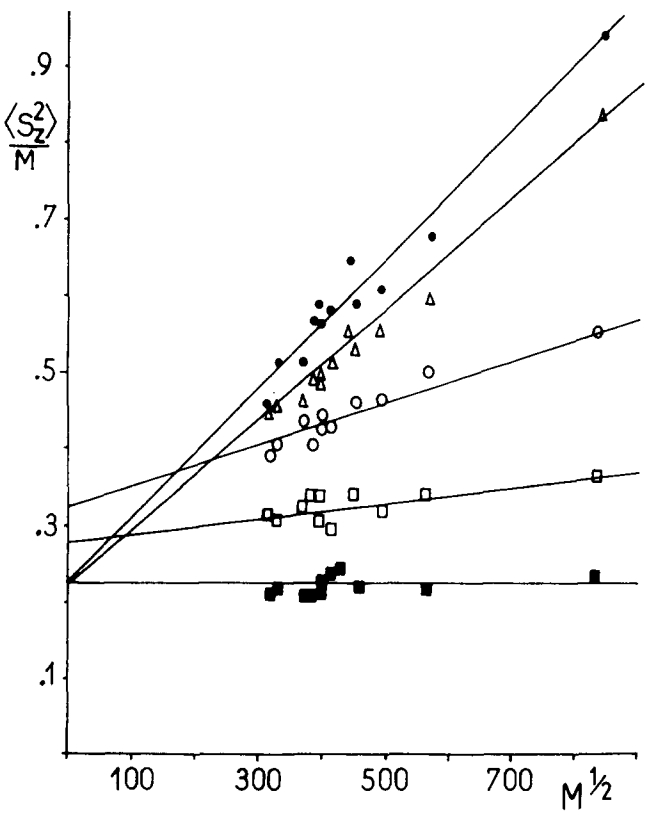

Figure 5 Plot of $\langle s^2 \rangle_z/M_w$ (10^{-16} cm^2 g^{-1} mol) as a function of $M_w^{1/2}$ (g$^{1/2}$ mol$^{-1/2}$); same symbols as in *Figure 2*

enough to 1 to apply relation (6) to $M_{w,PS}$. These corrected values compare well to M_w. The reliability of the conversion is reinforced by the experiments carried out with double detection. We therefore take $M_{w,PS,corr}$ as a fair approximation for further s.e.c. characterization of PVDF (see part 2).

UNPERTURBED DIMENSIONS AND THERMODYNAMIC INTERACTIONS

Scaling-law exponents ν and ν' in relations (2) and (3) are theoretically related by $\nu' = 1 - \nu$, in rough agreement with the data in *Table 4*. The inconsistency of the viscosity data[10], where a should be between $3\nu - 1$ and $2\nu - 1/2$, has already been mentioned. The results in DMAc where most data have been accumulated seem in this respect the most reliable ($a \simeq 3\nu - 1$). Since the polymolecularity indices do not vary widely between samples with mean values $I_p \simeq 2.0$ and $I_{p+1} \simeq 2.2$, we use these values directly to derive similar averages on $\langle s^2 \rangle_z$ and M_w and to calculate unperturbed dimensions and thermodynamic interactions.

Unperturbed dimensions

To eliminate the influence of excluded volume in non-theta solvents, we use the Stockmayer–Fixman procedure[11] and plot (*Figure 5*) $\langle s^2 \rangle_z/M_w$ as a function of $M_w^{1/2}$. The plot is reasonably linear and the extrapolation

in different solvents leads to:

$$(\langle s^2\rangle_z/M_w)_{\text{unperturbed}} = (0.25 \pm 0.05) \times 10^{-16}\ \text{cm}^2\ \text{g}^{-1}\ \text{mol}$$

Taking into account $I_{p+1} \simeq 2.2$ one can correct for polymolecularity to get:

$$(\langle s^2\rangle/M)_{\text{unperturbed}} = (0.11 \pm 0.02) \times 10^{-16}\ \text{cm}^2\ \text{g}^{-1}\ \text{mol}$$

From the Flory–Fox relation[12]:

$$[\eta] = \phi'\langle s^2\rangle^{3/2}/M$$

we can also use a plot of $[\eta]/M^{1/2}$ as a function of $M^{1/2}$ (*Figure 6*) and the accepted value $\phi' = 2.5 \times 10^{23} \times 6^{3/2} = 3.6 \times 10^{24}$ mol to get another value of $\langle s^2\rangle/M = 0.14 \times 10^{-16}\ \text{cm}^2\ \text{g}^{-1}$ mol, which is less defined from the point of view of polymolecularity but in satisfactory agreement with the former.

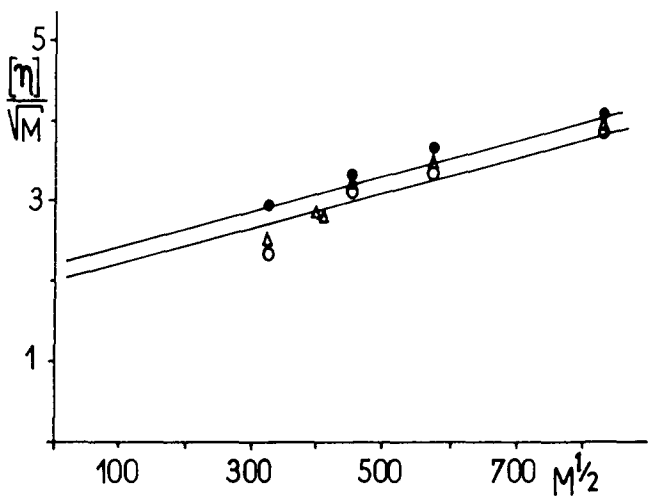

Figure 6 Plot of $[\eta]/M_w^{1/2}$ (10^{-3} dl $g^{-3/2}$ $mol^{1/2}$) as a function of $M_w^{1/2}$ ($g^{1/2}$ $mol^{-1/2}$); same symbols as in *Figure 2*

Characteristic ratio C_∞ and conformations of PVDF

From the monomer molecular mass $m = 64$ g mol^{-1} and C–C bond length $l = 1.54$ Å, one can calculate:

$$C_\infty = \frac{\langle h^2\rangle}{nl^2} = \frac{3m}{l^2}\left(\frac{\langle s^2\rangle}{M}\right)_{\text{unperturbed}} = 8.9 \pm 2$$

For a vinylic chain with symmetrically hindered rotation one has:

$$C_\infty = \frac{1+\cos\theta}{1-\cos\theta}\,\frac{1+\langle\cos\phi\rangle}{1-\langle\cos\phi\rangle}$$

where θ is the tetrahedral angle ($\cos\theta = 1/3$) and $\langle\cos\phi\rangle$ the mean angle of internal rotation. The computed value $\langle\cos\phi\rangle = 0.66 \pm 0.03$ can be expressed in term of the probability for *trans* and *gauche* rotameric isomers:

$$\langle\cos\phi\rangle = p(t)\cos(0°) + p(g)\cos(\pm 135°)$$
$$= (1 + \sqrt{2}/2)p(t) - \sqrt{2}/2$$

Thus

$$p(t) = 1 - p(g) = 0.80$$

This value fits closely to an equal-probability mixture of the three molecular conformations; all *trans* ($p(t) = 1$), $TGT\bar{G}$ ($p(t) = \frac{1}{2}$) and $T_3GT_3\bar{G}$ ($p(t) = \frac{3}{4}$), detected in the different crystal structures of PVDF[1].

Thermodynamic interaction parameters χ

Flory's theory[13] gives a simple relation between A_2 and χ:

$$A_2 = (\tfrac{1}{2} - \chi)\bar{v}_2^2/V_1F(x) \qquad (8)$$

where $\bar{v}_2$ is the partial specific volume of the polymer (here taken as the bulk specific volume $\bar{v}_2 = 0.552$ cm^3 g^{-1}), V_1 the molar volume of the solvent and $F(x)$ a function of the expansion factor α through $x = (2\alpha^2 - 1)$. At low x, $F(x)$ is expressed by the expansion:

$$F(x) = 1 - \frac{x}{2!2^{3/2}} + \frac{x^2}{3!3^{3/2}}$$

Table 7 Thermodynamic interaction parameter χ

	DMSO		DMF		DMAc		NMP		DMPU		HMPT	
Sample	$F(x)$	χ	$F(x)$	χ	$F(x)$	χ	$F(x)$	χ	$F(x)$	χ	$F(x)$	χ
A1	0.98	0.49	0.97	0.46	0.92	0.15	0.80	0.013	0.88	−0.22	0.89	−0.66
A2	0.97	0.49	0.95	0.46	0.91	0.16	0.80	0.013	0.82	−0.2		
A3	0.98	0.49	0.94	0.46	0.88	0.19	0.79	0.08	0.82	−0.15		
A4	0.98	0.49	0.93	0.47	0.89	0.20	0.78	0.08	0.8	−0.12		
A5	0.98	0.49	0.93	0.47	0.87	0.20	0.78	0.08	0.79	−0.12		
A6	0.95	0.49	0.93	0.47	0.87	0.22	0.78	0.03	0.79	−0.12		
S1010	0.93	0.49	0.93	0.47	0.87	0.22	0.78	0.05	0.8	−0.15		
A7	0.96	0.49	0.92	0.47	0.86	0.25	0.77	0.05	0.78	−0.15	0.82	−0.62
S1012	0.94	0.49	0.92	0.47	0.85	0.26	0.76	0.07	0.78	−0.08		
A8	0.96	0.50	0.90	0.48	0.83	0.28	0.73	0.09	0.76	−0.07		
A9	0.93	0.50	0.88	0.49	0.80	0.34	0.81	0.15	0.77	−0.01	0.77	−0.4
$\langle\chi\rangle$		0.49 ± 0.01		0.47 ± 0.02		0.25 ± 0.10		0.10 ± 0.05		−0.15 ± 0.10		−0.50 ± 0.15
χ_{ic}		−1.0		−1.5		−1.3		−1.5		−1.5		−1.7

$\langle\chi\rangle$ is the average on the samples and χ_{ic} is the χ measured by inverse gas chromatography

We have calculated x for all samples and solvents using for α^2 the ratio of the actual $\langle s^2 \rangle_z$ to the unperturbed value derived from the Stockmayer–Fixman extrapolation in *Figure 4*. The corresponding values of $F(x)$ and χ are given in *Table 7*. A comparison with the values calculated from inverse gas chromatography[14] illustrates the difficulty of extrapolating these values to solution properties.

CONCLUSIONS

A complete characterization of solution properties of PVDF has been performed. DMSO appears very close to a theta solvent and DMPU as an easy-to-handle good solvent for LS experiments. A conversion formula from PS calibration to true M_w has been established for s.e.c. in NMP/LiBr. The characteristic ratio of this polymer has been calculated and reflects the high content of *trans* isomers in agreement with the chain conformation in the known crystalline forms of PVDF.

REFERENCES

1 Lovinger, A. J. in 'Developments in Crystalline Polymers, 1' (Ed. D. C. Bassett), Applied Science, London, 1981, Ch. 5
2 Stillwagon, L. E. *Org. Coatings, Appl. Polym. Sci. Proc.* 1983, **48**, 780
3 Welch, G. J. *Polymer* 1974, **15**, 429
4 Ali, S. and Raina, A. K. *Makromol. Chem.* 1978, **179**, 2925
5 Lutringer, G., Meurer, B. and Weill, G. *Polymer* 1991, **32**, 884
6 Galin, J. C., Lutringer, G. and Galin, M. *J. Appl. Polym. Sci.* 1989, **37**, 487
7 Grubisic, Z., Rempp, P. and Benoit, H. *J. Polym. Sci., Polym. Lett.* 1967, **5**, 753
8 Breda, A. private communication
9 Mori, S. *Anal. Chem.* 1983, **55**, 2414
10 Weill, G. and des Cloizeaux, J. *J. Physique.* 1979, **40**, 99
11 Stockmayer, W. H. and Fixman, M. *J. Polym. Sci.* (*C*) 1963, **1**, 137
12 Flory, P. J. and Fox, T. G. *J. Am. Chem. Soc.* 1951, **73**, 1904
13 Flory, P. J. 'Principles of Polymer Chemistry', Cornell University Press, Ithaca, NY, 1953
14 Galin, M. and Maslinko, L. *Macromolecules* 1985, **18**, 2192